doi:10.1016/j.jmb.2005.08.061 J. Mol. Biol. (2005) 353, 642–654

JMB

Available online at www.sciencedirect.com

SCIENCE DIRECT®

ELSEVIER

Towards a Structural Understanding of the Fibrillization Pathway in Machado-Joseph's Disease: Trapping Early Oligomers of Non-expanded Ataxin-3

Luís Gales[1], Luísa Cortes[2], Carla Almeida[2], Carlos V. Melo[2] Maria do Carmo Costa[3], Patrícia Maciel[3], David T. Clarke[4] Ana Margarida Damas[1] and Sandra Macedo-Ribeiro[2]*

[1]*ICBAS-Instituto de Ciências Biomédicas de Abel Salazar and IBMC-Instituto de Biologia Molecular e Celular Universidade do Porto, Portugal*

[2]*Macromolecular Crystallography Group, Center for Neuroscience and Cell Biology (CNC), 3004-517 Coimbra, Portugal*

[3]*Health and Life Sciences Research Institute/School of Health Sciences, University of Minho, Campus de Gualtar 4710-057 Braga, Portugal*

[4]*CCLRC Daresbury Laboratory Daresbury, Warrington WA4 4AD, UK*

**Corresponding author*

Machado-Joseph's disease is caused by a CAG trinucleotide repeat expansion that is translated into an abnormally long polyglutamine tract in the protein ataxin-3. Except for the polyglutamine region, proteins associated with polyglutamine diseases are unrelated, and for all of these diseases aggregates containing these proteins are the major components of the nuclear proteinaceous deposits found in the brain. Aggregates of the expanded proteins display amyloid-like morphological and biophysical properties.

Human ataxin-3 containing a non-pathological number of glutamine residues (14Q), as well as its *Caenorhabditis elegans* (1Q) orthologue, showed a high tendency towards self-interaction and aggregation, under near-physiological conditions. In order to understand the discrete steps in the assembly process leading to ataxin-3 oligomerization, we have separated chromatographically high molecular mass oligomers as well as medium mass multimers of non-expanded ataxin-3. We show that: (a) oligomerization occurs independently of the poly(Q)-repeat and it is accompanied by an increase in β-structure; and (b) the first intermediate in the oligomerization pathway is a Josephin domain-mediated dimer of ataxin-3. Furthermore, non-expanded ataxin-3 oligomers are recognized by a specific antibody that targets a conformational epitope present in soluble cytotoxic species found in the fibrillization pathway of expanded polyglutamine proteins and other amyloid-forming proteins. Imaging of the oligomeric forms of the non-pathological protein using electron microscopy reveals globular particles, as well as short chains of such particles that likely mimic the initial stages in the fibrillogenesis pathway occurring in the polyglutamine-expanded protein. Thus, they constitute potential targets for therapeutic approaches in Machado-Joseph's disease, as well as valuable diagnostic markers in disease settings.

Keywords: SCA3; self-assembly domain; neurodegenerative; polyglutamine; amyloid

Introduction

Several human disorders are caused by trinucleotide expansions in a heterogeneous group of genes.[1] CAG expansions leading to increased polyglutamine repeats within the affected proteins are responsible for nine slowly progressive disorders collectively known as polyglutamine (poly(Q)) diseases. Despite ubiquitous expression of both the normal and disease proteins throughout the

Abbreviations used: EM, electron microscopy; HMM oligomers, high molecular mass oligomers; MJD, Machado-Joseph's disease; MJDL-CE, *Caenorhabditis elegans* ataxin-3 like protein containing a single glutamine residue (1Q) in the region corresponding to the polyglutamine domain; MJD1-1, human ataxin-3 isoform 2 containing 14 glutamine residues (14Q) in the repeat region; poly(Q), polyglutamine; UIM, ubiquitin interacting motif; ThT, thioflavin T; NIs, neuronal inclusions.

E-mail address of the corresponding author: sribeiro@ibili.uc.pt

brain and other tissues, only a particular subset of neurons is selectively affected in each disease. Nuclear and sometimes cytoplasmatic neuronal inclusions (NIs) containing the mutant proteins, are now clearly established as the identifying fingerprint of poly(Q) diseases.[2,3] Longer poly(Q) repeats cause more severe disease symptoms, implying that the degree of toxicity is directly proportional to the size of the repeat.

The structural and functional effects of poly(Q) expansions in the affected proteins as well as the mechanisms of polyglutamine toxicity are still not clear. An enormous research effort has been put into understanding the structure of polyglutamine and the structural changes induced by polyglutamine expansion.[4,5] Current experimental data show that, independently of the repeat length, monomeric polyglutamine sequences exist predominantly in a random coil conformation. A conformational transition occurs upon aggregation: in close connection with the pathological threshold in polyglutaminopathies, the tendency to aggregate into β-rich fibrillar structures increases with poly(Q) length.[6] The amyloid nature of these polyglutamine insoluble structures has been demonstrated by numerous experiments *in vitro*[7–9] and *in vivo*.[7,10] Furthermore, poly(Q) aggregates are recognized by "pan-amyloid" antibodies able to associate with generic amyloid epitopes in fibrils formed from a diverse number of proteins.[11] Whether the cellular toxicity is triggered by the pathogenic disease protein alone, by the putative intermediates of the fibrillization pathway, or by the soluble mature fibrils, is still a matter of debate.[12] In this line, protofibrillar intermediates in polyglutamine proteins have already been identified.[9,13,14] Because poly(Q) aggregates exhibit most of the characteristic features of amyloid structures,[15] the formation of the mature fibrils probably occurs *via* early assembly intermediates that have been implicated as the toxic species responsible for cell dysfunction and neuronal loss.[16,17]

Expanded ataxin-3 is found in nuclear inclusions[18] in Machado-Joseph's disease (MJD), a disease that has the highest prevalence in the Azores islands of Flores and Sao Miguel. Although the precise cellular role(s) of ataxin-3 are still not fully characterized, its function as a polyubiquitin hydrolase and its role as a suppressor of poly(Q)-induced neurodegeneration is just starting to be unveiled.[19–22] Ataxin-3 is a modular protein comprised of a conserved N-terminal Josephin domain,[23,24] containing the catalytic cysteine residue, followed by two ubiquitin interacting motif (UIM) domains and the poly(Q) repeat domain. Four different transcript variants of the human protein (Figure 1) have been identified, although their functional relevance and expression *in vivo* are still unknown.[25] As observed in other polyglutaminopathies, there is a threshold polyglutamine

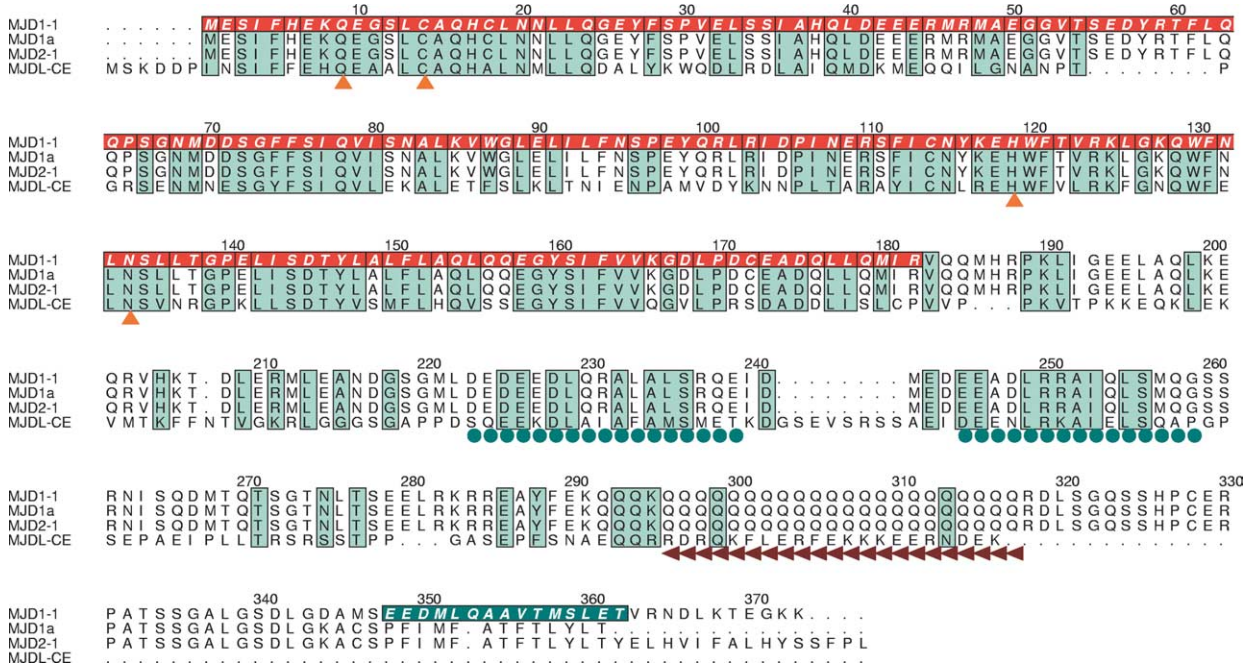

Figure 1. Sequence alignment of human and *C. elegans* ataxin-3. Three of the four known human ataxin-3 isoforms: MJD1-1 (SwissPROT: P54252 variant VSP_002784), MJD2-1 (SwissPROT: P54252) and MJD1a (SwissPROT: P54252 variant VAR_013689), are compared with the *C. elegans* ataxin-3-like protein (MJDL-CE, SwissPROT: O17850). Identical residues are shaded in light green. The catalytic Josephin domain is boxed in red and the UIM domains are indicated by filled blue circles below the alignment. Notice that only ataxin-3 variant MJD1-1 contains a third UIM domain (boxed in blue) after the poly(Q) tract (red left-arrow triangles below the alignment). Numbering refers to the MJD1-1 amino acid sequence. Residues important for catalysis are highlighted by orange triangles below the alignment. Multiple sequence alignment was preformed with TCOFFEE[60] and the Figure was prepared with ALSCRIPT.[61]

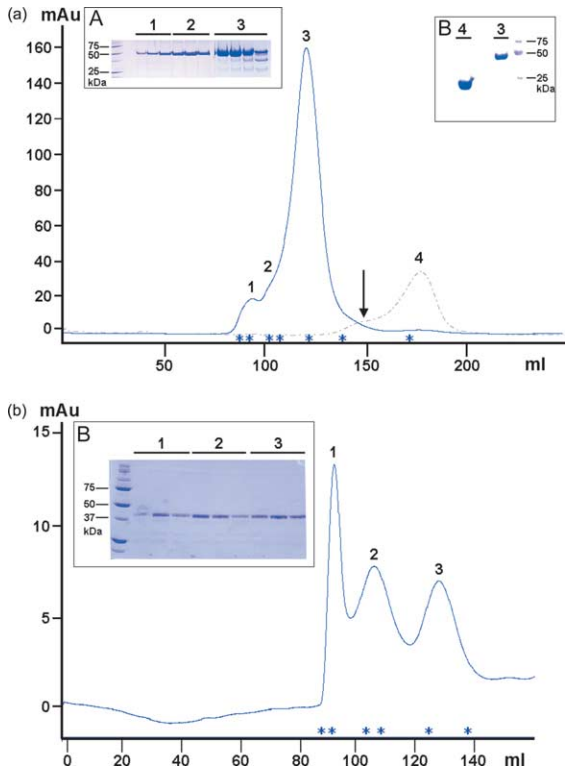

Figure 2. Non-expanded ataxin-3 oligomerizes under near-physiological conditions. (a) Monomeric human ataxin-3 can be separated from high molecular mass oligomers by size-exclusion chromatography (Hiprep 26/60 Sephacryl S-200 HR). Elution profiles of native human ataxin-3 eluted from the HisTrap column with 100 mM (black line) imidazole, monitored at 280 nm. The elution profile, in combination with the SDS-PAGE analysis of the isolated fractions (inset A), indicate that the purified protein exists in different oligomeric forms. The protein elutes with a predominant monomeric peak (peak 3), although partially contaminated with the other oligomeric forms (peaks 1 and 2). The oligomeric species partition into two overlapping peaks, one eluting around 106 ml (peak 2), possibly representing a mixture of homo-multimers with different subunit compositions, and the void volume eluate (peak 1), representing higher-order soluble ataxin-3 oligomers. Monomeric ataxin-3 elutes faster than expected for a globular 44 kDa protein, but this behaviour might reflect the non-spherical shape of this protein.[8] For comparison purposes, the elution profile of the catalytic Josephin domain (peak 4, predicted molecular mass 23 kDa) is also shown (broken black line); the black arrow highlights the shoulder preceding the major peak of the Josephin domain, representing Josephin dimers (see the text and Figure 3). The purified monomeric form of full-length ataxin-3 and the Josephin domain alone were concentrated to ~10 mg/ml and analysed by SDS-PAGE under reducing conditions (inset B). (b) Size-exclusion chromatography (Hiprep 26/60 Sephacryl S-200 HR) elution profile of MJDL-CE, monitored at 280 nm. The protein applied to the column was eluted from the HisTrap column with 500 mM imidazole, and it is separated into three well-resolved peaks, of high molecular mass oligomers (peak 1), multimers (peak 2), and monomers (peak 3). Fractions of 5 ml were collected and analysed by SDS-PAGE (12% polyacrylamide gels) (inset A). All gels are stained with Coomassie brilliant blue. Asterisks (*) denote the positions of the molecular mass standards, from left to right: blue dextran (2000 kDa), thyroglobulin (669 kDa), catalase (232 kDa), aldolase (158 kDa), bovine serum albumin (67 kDa), ovalbumin (43 kDa), and chymotrypsinogen (25 kDa).

length (14–40 residues) for ataxin-3, below which the pathways leading to selective neural loss are not triggered within the human lifespan.[26] Remarkably, it has been shown that non-expanded protein can also form amyloid fibrils with increased β-sheet structure upon partial unfolding induced by increased temperature and pressure,[27,28] as well as by chemical denaturation.[29]

In order to understand the structural mechanisms that link polyglutamine expansion with disease, and to clarify the role of the poly(Q) repeats in ataxin-3 aggregation, we expressed and purified the homologous ataxin-3 protein from *Homo sapiens* (14Q), and the orthologue protein from *Caenorhabditis elegans* (26.9% identity, 1Q). Human ataxin-3, as well as heterologous *C. elegans* protein form, under near-native conditions, high molecular mass (HMM) oligomers and smaller multimers that we isolated chromatographically from the monomeric forms for further characterization.

Results

Non-expanded ataxin-3 self-associates to form soluble high molecular mass oligomers

We have cloned and over-produced in *Eschrerichia coli* the isoform MJD1-1 (Figure 1) of non-expanded human ataxin-3, with a poly(Q) tract of 14 residues, and the *C. elegans* ataxin-3-like protein (MJDL-CE, Figure 1), containing a single glutamine residue in the region corresponding to the poly(Q). The *C. elegans* ataxin-3-like protein and the human protein display around 27% identity, being mostly similar within the catalytic Josephin domain (43% identity).

Gel-filtration chromatography analysis of the ataxin-3 containing fractions, eluted from the metaloaffinity column, showed that for both human (14Q) and *C. elegans* (1Q) proteins soluble oligomeric and monomeric forms coexist. These results indicate that ataxin-3 is able to self-assemble into homo-multimeric species of different sizes, independently of the length of the poly(Q)-tract (Figure 2). The gel-filtration profile of protein fractions purified from the HisTrap column showed that human ataxin-3 separates into a well-resolved predominant peak containing monomeric protein (Figure 2(a), peak 3), and two overlapping oligomeric fractions (Figure 2(a), peaks 1 and 2). In contrast, MJDL-CE separates into three major well-resolved peaks (see Figure 2(b)) that we called HMM oligomers (peak 1), multimers (peak 2), and monomers (peak 3). Despite the fact that MJDL-CE contains a single glutamine rersidue, this protein

forms a higher percentage of oligomeric species, and it is less stable than the human protein, showing a much greater tendency towards precipitation and degradation.

Although the predicted molecular mass of human ataxin-3 is ~44 kDa (Figure 2(a), inset A), the lower molecular mass peak (peak 3) elutes from the gel-filtration column before the 67 kDa molecular mass marker. This behaviour is observed also for monomeric MJDL-CE (Figure 2(b), peak 3; expected molecular mass ~39 kDa). The anomalous migration observed for the two proteins likely indicates that both MJD1-1 and MJDL-CE display an overall elongated shape, similar to what has been observed for isoform MJD1a (Figure 1).[8]

To further evaluate the oligomerization state of the soluble ataxin-3 aggregates, aliquots from the peaks separated by gel-filtration chromatography were crosslinked with glutaraldehyde to fix the aggregation state of the proteins, allowing their analysis under denaturing conditions by SDS-PAGE (Figure 3). This confirmed that the lower molecular mass peaks (Figure 2(a) and (b), peak 3) do correspond to monomeric species. The faint band of dimers observed upon longer incubations of monomeric ataxin-3 with glutaraldehyde (Figure 3(a)), likely represents non-specific crosslinking effects resulting from random collisions of monomers. Similar results are observed upon crosslinking of lysozyme under identical experimental conditions (data not shown). The MJD1-1 protein eluting just before the monomer, with a calculated molecular mass of 140 kDa (Figure 2(a), peak 2), is likely enriched in ataxin-3 dimers as

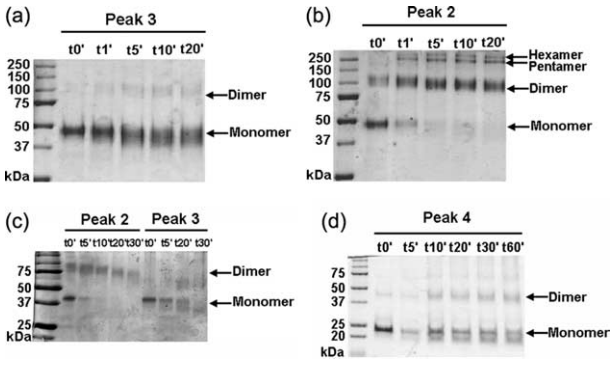

Figure 3. Ataxin-3 self-assembles into multimeric species composed of dimers, pentamers and hexamers. Crosslinking was performed with 0.02% glutaraldehyde for human ataxin-3 fractions collected from (a) peak 3 and (b) peak 2 and for the *C. elegans* ataxin-3 fractions collected from (c) peaks 2 and 3. The protein was incubated at room temperature and 10 μl aliquots were collected at the indicated time-points, the reaction was stopped by adding sample buffer and heating to 100 °C for 5 min. (d) Crosslinking of protein isolated from the small shoulder preceding the major peak of the Josephin domain, indicating that this domain alone is able to oligomerize. Samples were analyzed by SDS-PAGE and the gels in (a), (b) and (d) were stained with Coomassie brilliant blue. The gel in (c) was stained with silver.

observed by the appearance of a predominant ~100 kDa species on SDS-PAGE, accompanied by the simultaneous disappearance of the 44 kDa band, after crosslinking with glutaraldehyde (Figure 3(a)). Those dimers are not homogeneous and consistently appear contaminated with two discrete bands with molecular mass greater than 250 kDa, possibly representing MJD1-1 pentamers and hexamers, and for this reason we refer to these species as multimers. Those multimers of the human protein could not be fully separated from the other oligomeric species and are very unstable, quickly converting into higher molecular mass structures (see Supplementary Data, Figure 1). Crosslinking analysis of the MJDL-CE intermediate peak (Figure 2(b), peak 2) indicates that it is also a dimer separating very well from higher molecular mass oligomers (Figure 3(c)). In contrast, crosslinking of the HMM oligomers (Figure 2(a) and (b); peak 1) yielded species that did not enter the gel, even when lower concentrations of glutaraldehyde were used (data not shown). Those species have apparent molecular mass of 300–600 kDa, as calculated by comparison with known molecular mass standards in gel-filtration chromatography.

Oligomer formation seems to be an intrinsic property of ataxin-3 proteins, independent of the length of the polyglutamine domain. In agreement, *in vitro* cell studies with cellular models expressing expanded and non-expanded ataxin-3 have shown that both proteins form large macromolecular complexes.[30] Indeed, under the same experimental conditions we can observe the formation of HMM oligomers of mouse (6Q) and chicken (7Q) ataxin-3 homologues (S. M.-R., unpublished results). Considering that the domain with the highest degree of conservation across species is the Josephin domain, we have decided to further investigate the properties of this catalytic domain of human ataxin-3. The Josephin domain migrates with the predicted molecular mass on the gel-filtration column (Figure 2(a), inset B), as expected from a globular protein, and in agreement with previously reported experimental data.[23,31] However, no HMM oligomeric species are observed during the purification of the Josephin domain alone, although the presence of a small shoulder preceding the major peak (Figure 2(a), peak 4), indicates the presence of a small percentage of dimers that cannot be separated completely from the monomeric forms. The partial dimerization of the Josephin domain was confirmed by crosslinking with glutaraldehyde (Figure 3(d)). Under partially denaturing conditions, we did observe precipitation of the protein into amyloid-like structures capable of binding Congo red (S. M.-R., unpublished results) as reported recently.[31]

Altogether, our results provide evidence that non-expanded ataxin-3 has an intrinsic propensity to oligomerize, and that oligomerization is not mediated by direct poly(Q) interactions. Furthermore, the fact that we could observe the formation of dimers of both full-length human and *C. elegans*

ataxin-3, and that the truncated human Josephin domain alone shows propensity for dimerization, clearly implicates this highly conserved domain in ataxin-3 dimerization. Further oligomerization events seem to be mediated and/or induced, at least under our experimental conditions, by the other protein domains.

Circular dichroism analysis suggests that a conformational change occurs upon oligomerization

To further characterize the nature and properties of the oligomeric forms of ataxin-3, a combination of methods has been used. They include binding to histological dyes, such as thioflavin T (ThT), and circular dichroism (CD) to elucidate the constituent secondary structure.

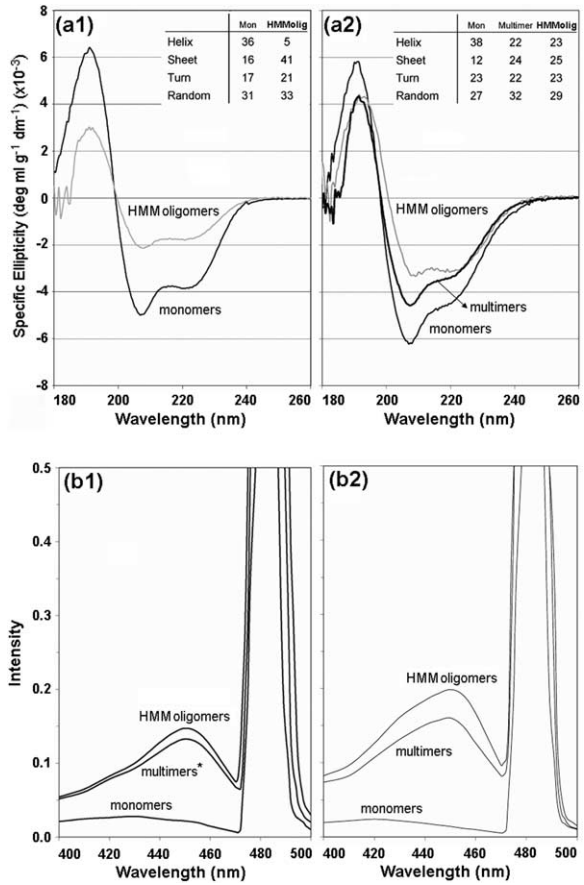

Figure 4. Ataxin-3 early oligomers are β-rich amyloid-like structures. (a) The CD spectra of (a1) human and (a2) *C. elegans* ataxin-3 in the monomeric and oligomeric forms. The secondary structure content was calculated using the Contin method and is displayed (in %). The β-sheet conversion accompanies protein aggregation and is more marked for human ataxin-3. (b) Thioflavin-T binding assays of (b1) human and (b2) *C. elegans* ataxin-3. The oligomeric species are all thioflavin-T positive, reflecting the amyloid-like properties of those early ataxin-3 aggregates. Multimers (*) of human ataxin-3 are a heterogeneous mixture of different oligomerization states (see Supplementary Data, Figure 1).

The secondary structure of MJD1-1 in the monomeric and in the oligomeric forms was determined by CD spectroscopy. The spectra of the monomeric form of the human protein display a high content of α-helix, 36%, in agreement with previous results,[8,23] and a relatively lower percentage of β-sheet (16%), and β-turn (17%, Figure 4(a)). There is also a significant fraction of random coil conformation (31%), suggesting the presence of a flexible portion of the protein, which is in agreement with previous studies.[23] The relative proportion of α-helix, β-sheet and β-turn is relatively well conserved for MJDL-CE, indicating a conservation of the overall secondary structure for this ataxin-3 ortholog (Figure 4(a)).

Oligomerization induces important alterations in the secondary structure of the protein. CD analysis of the HMM MJD1-1 oligomers, that display greater homogeneity than the multimeric species after a freeze–thaw cycle (see Supplementary Data, Figure 1), show that there is a drastic reduction in the α-helix content accompanied by the proportional increase in β-sheet structure. The β-turn and random coil contents show minor alterations upon oligomerization (Figure 4(a)). The *C. elegans* ataxin-3-like protein (1Q) displays the same behaviour as the human ataxin-3 (14Q) (increase in β-sheet and decrease in α-helix content), although to a significantly lesser extent. The HMM oligomers, and even the earlier multimeric species of both the human and *C. elegans* proteins, are ThT-positive (Figure 4(b)). This fluorescent dye is known to bind β-rich fibrillar structures.

From our observations, freezing (at −80 °C) and thawing the protein between purification steps can increase the proportion of HMM oligomers up to 90% of the total soluble MJD1-1 ataxin-3 purified. Furthermore, it consistently forms fibrillar precipitates upon thawing. This susceptibility towards aggregation induced by freezing has been reported for poly(Q)-containing peptides.[6] Those ataxin-3 precipitates bind Congo red, a known reporter of repetitive β-structures, and display red-green birefringence characteristic of amyloid-like fibrils (Figure 5(a)). Electron microscopy analysis revealed the presence of elongated fibrils and a small number of granular aggregates (Figure 5(b)). These structures are reminiscent of the precursor aggregates (protofibrils) that precede formation of amyloid fibrils.[16,32,33]

Seeding effects in ataxin-3 aggregation

The aggregation progress of poly(Q) proteins can be followed consistently using techniques such as CD spectroscopy, HPLC, light-scattering and ThT fluorescence.[34] In this work, we monitored the polymerisation kinetics of MJD1-1 by ThT fluorescence. Furthermore, we evaluated the seeding effect in the aggregation progress by adding, at time zero, a small amount (4%, w/w) of dimers and of HMM oligomers (10%, w/w). We observed that there is an initial lag phase, which is reduced significantly by seeding with pre-formed dimers or

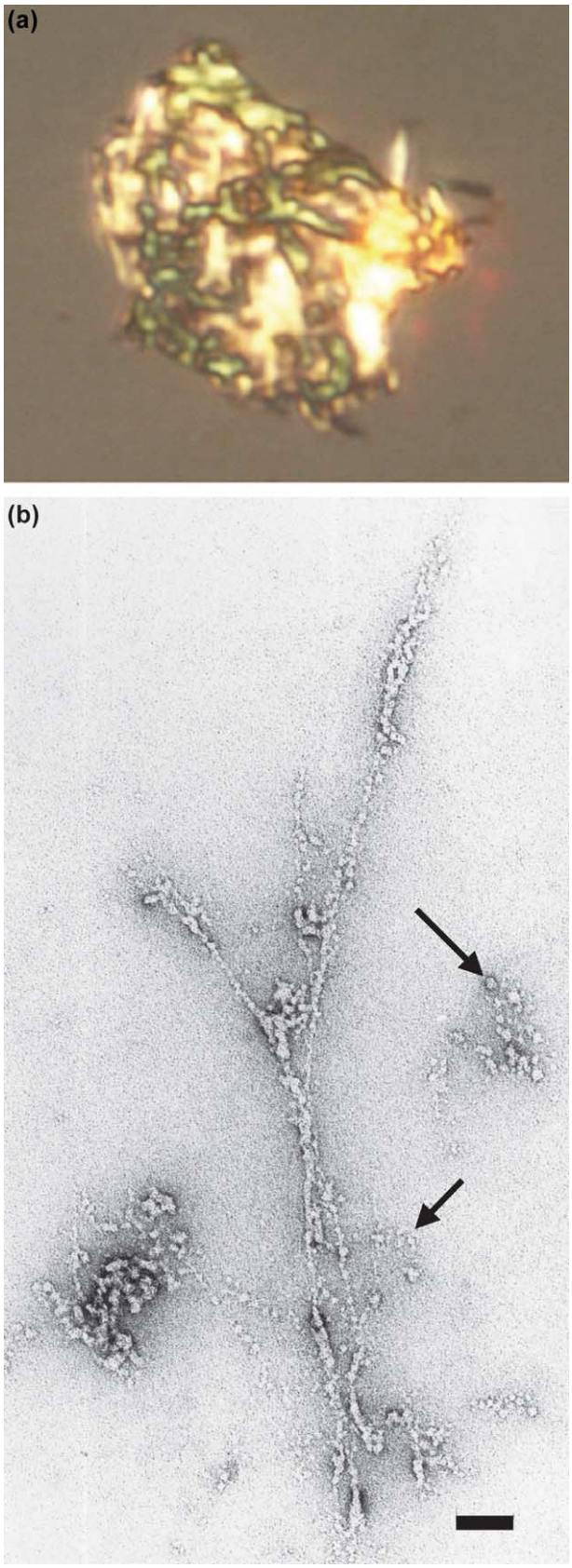

Figure 5. Amyloid-like properties of ataxin-3 insoluble aggregates. Non-expanded human ataxin-3 precipitates into amyloid-like structures (a) as detected by red-green birefringence upon binding Congo red and (b) electron micrographs of the negatively stained insoluble material. The fibril diameter is 8–12 nm. The short and curly fibrils are characteristic of protofibrils or "immature" amyloid fibrils. Arrows show granular oligomeric structures. The scale bar represents 100 nm.

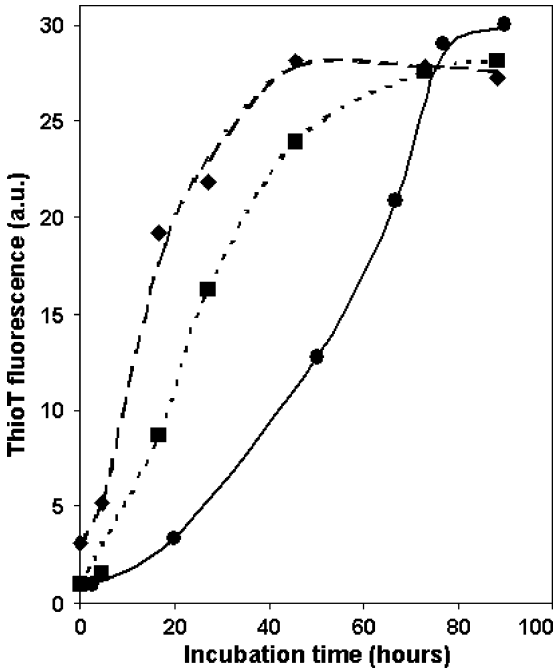

Figure 6. Dimers and HMM oligomers seed human ataxin-3 fibril formation. Aggregation kinetics at 37 °C of human ataxin-3, as monitored by thioflavin-T fluorescence. Polymerisation progress at pH 7.5 without seed (•), with addition at time 0 of 4% (w/w) of preformed dimers (■), and with addition at time 0 of 10% (w/w) of high molecular mass soluble oligomers (♦). Aggregation follows a nuclear-growth model with a marked seeding effect.

HMM oligomers, followed by a rapid growth phase (Figure 6). This behaviour is typical of poly(Q) aggregation *in vitro*,[35] and it suggests a nuclear-growth polymerisation model.

Without the addition of preformed oligomers, we observed a complete time-course of aggregation of around 90 h at 37 °C and an initial lag phase of less than 10 h. A previous work on the MJD1a variants of ataxin-3 (Figure 1) containing 15, 28 and 50 residues in their glutamine tract, reported no aggregation, as monitored by ThT fluorescence, within 24 h for ataxin-3(15Q) and ataxin-3(28Q), and aggregation to near-completion of the pathological ataxin-3(50Q) in 24 h.[36] Indeed, we have observed for the MJD1-1 variant that during the first 24 h of incubation at 37 °C the increase of ThT fluorescence is relatively small. This initial stage is followed by a rapid growth phase in the case of the MJD1-1 variant, which can be clearly monitored by ThT fluorescence.

The complete time-course of polymerisation of

MJD1-1, and the length of the initial lag phase in particular, are very sensitive to seeding with dimers, multimers (data not shown) and HMM oligomers. The strong effect of adding a small amount of dimers at time zero suggests that nucleation involves either the refolding of the monomer, as was proposed by Chen and co-workers based on the aggregation kinetics of poly(Q) peptides,[34] or the formation of a dimer.

Transmission electron microscopy reveals the morphological characteristics of non-pathological ataxin-3 along the aggregation pathway

We are currently able to sample three distinct soluble oligomeric states of ataxin-3: non-globular monomers, multimers, and HMM oligomers. Those profiles are obtained consistently by gel-filtration chromatography, independently of the total concentration of ataxin-3. The HMM oligomers are rather homogeneous and remain stable upon storage at −80 °C. The multimers of human ataxin-3 are not particularly stable, converting quickly to higher molecular mass forms. The heterogeneity of the multimeric species is higher for the human than for the *C. elegans* protein.

The multimers of MJD1-1 were separated freshly by gel-filtration chromatography (Supplementary Data, Figure 1) and electron microscopy was used to examine the structure of isolated species in the individual peaks. Examination of the dimeric and of the oligomeric samples by transmission electron microscopy reveals the presence of spherical structures, although the corresponding diameter for the oligomers (~7 nm) (Figure 7) seems slightly larger than the diameter of the dimers (~6 nm) (Supplementary Data, Figure 1). Moreover, the

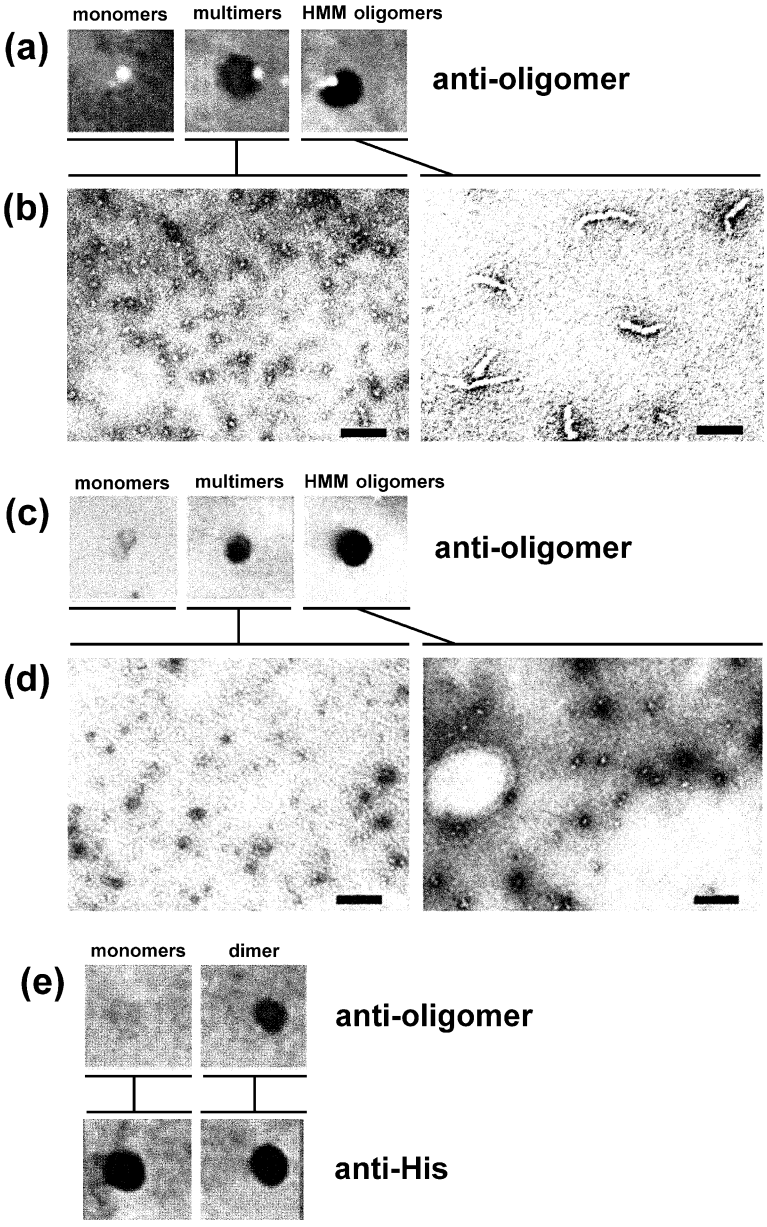

Figure 7. Spherical ataxin-3 oligomers are recognized by the anti-oligomer antibody. Characterisation of the different species of human recombinant ataxin-3 by dot blot analysis and electron microscopy. Soluble HMM oligomers, multimers and monomers of (a) human and (c) *C. elegans* recombinant ataxin-3 were applied to a nitrocellulose membrane and either probed with oligomer-specific antibody or anti-His antibody. Oligomer-specific antibody recognized all oligomeric species, and did not recognize monomers of recombinant ataxin-3, whereas anti-His antibody recognized all oligomerization forms of the recombinant protein (data not shown). EM images show the spherical morphology of (b) human and (d) *C. elegans* ataxin-3 oligomers (the scale bars represent 100 nm). (e) The anti-oligomer antibody recognizes an epitope present in the dimeric Josephin domain that is absent from the monomeric form of this protein.

oligomeric sample looks more heterogeneous and a residual population consisting of two or three aligned rod-like structures is present, which should correspond to the early stage of the elongation phase. The higher-order soluble aggregates have an elongated curvilinear structure. They are unbranched, with diameters of 7–9 nm and length up to 200 nm (Figure 7). These structures precede the formation of the protofilaments, which are mostly unbranched with a variable length up to 2 μm and a diameter of 8–12 nm (Figure 5). Also present along with these precursors of the mature fibrils are rod-like aggregates with diameters of 20–30 nm. The beaded morphology and width dimensions of the fibrils resemble those formed by expanded (78Q) ataxin-3.[8]

The MJDL-CE protein is separated by size-exclusion chromatography into three major well-resolved peaks (see Figure 2(b)), HMM oligomers, multimers and monomers. These three distinct samples were examined by electron microscopy. The monomeric sample was constituted by spherical structures and was, as expected, homogeneous (data not shown). The sample containing multimers was more heterogeneous and there were already aggregates, forming a few spherical structures (Figure 7). The HMM oligomers are formed by slightly elongated structures, with dimensions in the shorter direction of ~7 nm and in the longer direction ranging between 7 nm and 25 nm.

Characterisation of the oligomer-specific immunoreactivity

It has been shown recently that amyloid-β peptide, α-synuclein and poly(Q) peptides adopt a structural epitope found only in soluble oligomeric structures, which correlates with their cellular toxicity.[16,17,37]

Ataxin-3 multimers and HMM oligomers, bind the anti-oligomer antibody (Figure 7) independently of the length of the poly(Q) tract, joining the growing family of amyloidogenic intermediates that share a toxic conformation. This suggests that they might represent toxic intermediates with relevance for the pathogenesis of Machado-Joseph's disease, as shown for other amyloid-related degenerative diseases. Interestingly, the protein fraction enriched in a dimeric form of the Josephin domain (Figure 3(d)), also exposes an epitope clearly recognized by the anti-oligomer antibody that is absent from the monomeric form of the protein (Figure 7(e)). This indicates that dimerization of the Josephin domain is accompanied by a structural rearrangement that might constitute the first misfolding event of the ataxin-3 aggregation pathway.

Discussion

Poly(Q)-independent oligomerization

Amyloid is generally considered to be a non-native quaternary structure generated by defects in protein folding or clearance pathways. A diverse number of proteins with an abnormally long polyglutamine expansion display a strong tendency to form amyloid-like aggregates and are implicated in several progressive disorders. Ataxin-3, the smallest of these poly(Q) proteins, is associated with Machado-Joseph's disease.

Using human ataxin-3 containing a non-pathological number of glutamine residues (14Q), the *C. elegans* (1Q) orthologue we were able to (a) prove that the glutamine expansion is not essential for ataxin-3 amyloid fibril formation *in vitro*, and (b) trap for the first time early oligomers that are recognized by an oligomer-specific antibody, known to target soluble cytotoxic intermediates of many amyloidogenic proteins, including poly(Q) proteins.[16] Previous studies showed the formation of insoluble amyloid fibrils by non-expanded ataxin-3,[27–29] and specifically by the isolated Josephin domain.[31] Those studies, focused on the end-stage of ataxin-3 aggregation reactions, showed non-expanded protein aggregation following partial unfolding induced by pressure, temperature or chemical denaturation. The formation of amyloid fibrils upon partial protein denaturation has been demonstrated for a number of proteins, even those unrelated to amyloid pathologies.[38] In contrast, we have established near-physiological experimental conditions whereby non-pathological ataxin-3 forms soluble oligomeric structures. In agreement with previous results showing that the Josephin domain alone is able to form insoluble amyloid fibrils,[31] our results demonstrate that at least one of the protein oligomerization sites also maps to this catalytic domain. Even though this domain seems to be necessary for ataxin-3 oligomerization, our current CD data show also that the extent of the α-helix to β-sheet structure conversion upon oligomerization correlates with the length of the poly(Q) tract.

The heterogeneity of ataxin-3 oligomerization resembles very closely the data obtained for oligomerization of the chymotrypsin inhibitor 2 upon introduction of a four to ten residue poly(Q) stretch in the inhibitory loop.[39] As shown in the crystal structure of the isolated dimer, oligomerization occurred by a domain swapping mechanism,[40] and, although induced by the introduction of a polyglutamine repeat, was not mediated by the direct poly(Q) association.[41] All our present data indicate that a similar mechanism could induce the first steps in ataxin-3 oligomerization and that this association, most probably mediated by the Josephin domain, does not involve direct inter-glutamine interactions. The 3D domain swapping is a mechanism for proteins to form oligomers by exchanging identical domains,[42] and has been proposed as a possible mechanism leading to amyloid formation.[43] The presence of self-association regions with relevance for protein aggregation outside the poly(Q) tract has been described for ataxin-1.[44,45] Furthermore, it was demonstrated that high levels of wild-type ataxin-1 can cause degenerative phenotypes similar to those caused by

the expanded protein, indicating that ataxin-1 might have more than one stable conformation, and a certain percentage of the non-expanded protein does misfold into a pathogenic conformation.[46] This trend for the presence of self-association domains in proteins distant from the homopolymeric amino acid expansion has been observed for PABPN1, a protein associated with oculopharyngeal muscular dystrophy upon expansion of a polyalanine region.[47] It is becoming clear that although poly(Q) (as well as polyalanine) repeats are themselves toxic, the sequence and structure of the proteins carrying the poly(Q) tracts have important roles in defining the course and specificity of the disease.[48] Those sequences determine subcellular localization, specify interactions with other macromolecules within the cell and can certainly modulate the natural conformational heterogeneity of the protein.

Is a dimer formed by Josephin domain assembly the first intermediate in ataxin-3 oligomerization?

At physiological temperature, the aggregation of the monomeric form of human ataxin-3 (14Q) into amyloid-like structures takes around 90 h as monitored by the ThT binding assay. Moreover, it follows a sigmoidal-type time-response, suggesting that the nucleation is the controlling step of the aggregation pathway.[49] We have also observed a seeding effect when dimers, multimers or HMM oligomers are added to the monomeric form of the protein. Our results can be interpreted in light of a nuclear-growth polymerisation model,[49,50] consisting of a time-controlled nucleation phase during which only a small part of the soluble protein participates, followed by an elongation phase during which the soluble monomers are recruited into the growing fibre. Although our current experimental data do not allow us to completely trace the pathway of human ataxin-3 fibrillization, it is tempting to assume that the first oligomeric species in this pathway is a short-lived dimer, which quickly converts to larger, heterogeneous oligomeric species. The *C. elegans* ataxin-3 (1Q) dimer, although degrading very fast, could be well isolated from the HMM oligomers. We observed that freshly isolated dimers of MJDL-CE are ThT-positive (Figure 4(b)), display an increased β-sheet content (Figure 4(a)), and bind the anti-oligomer antibody. These results seem to hint that the first β-rich intermediate within the pathway of large-scale oligomerization is a dimer, formed by the full-length protein; specifically, by the Josephin domain. Dimerization implies a conformational change that exposes a specific epitope recognized by the anti-oligomer antibody. Further aggregation/extension events could involve other protein domains. We are presently pursuing experimental conditions that will allow us to optimize the separation and stabilization of the dimeric intermediates in order to further study their structural properties. Ataxin-3 dimers will clearly be preferential targets for therapy in MJD.

Biological relevance of ataxin-3 oligomerization: implications for Machado-Joseph's disease

We have demonstrated that non-expanded ataxin-3 has a natural tendency to oligomerize into β-rich ordered structures. Small spherical particles and larger curvilinear structures resulting from their linear association could be observed by electron microscopy. As observed for other amyloid forming proteins, we expect that ataxin-3 neurotoxicity arises from those soluble oligomeric species.[16,17,37] A number of reports stress the importance of oligomeric intermediates as the major cytotoxic species in various forms of amyloidogenesis,[51–54] even arguing that formation of insoluble inclusions might constitute a protective mechanism.[55]

Non-pathological recombinant ataxin-3 forms oligomers *in vitro*, displaying a pathogenic conformation, under physiological conditions. *In vivo*, both non-expanded and expanded forms of ataxin-3 have been detected within nuclear inclusions,[56–58] reinforcing the role of protein domains outside the expanded poly(Q)-tract in protein aggregation and disease pathogenesis. In the case of ataxin-3, one of the regions with propensity for oligomerization has been mapped to the Josephin domain. Thus, a tight control of the protein microenvironment by post-translational modifications, intracellular localization and/or interaction with specific macromolecular partners is thus crucial for controlling the formation of toxic intermediates by the non-expanded protein *in vivo*. Expansion of the polyglutamine, within the normal cell environment, probably triggers extremely small conformational changes[36] that persistently interfere with macromolecular interactions, thus continuously inducing the exposure of protein regions with high propensity to misfold and oligomerize. In agreement, polyglutamine expansion diseases are generally late-onset, reflecting long *in vivo* lag phases. Upon aging, the ability of the cell to deal with abnormal proteins decreases and favours the accumulation of toxic intermediates that induce cell damage.

It is our working hypothesis that while for the disease protein oligomerization can occur under physiological conditions, similar changes can occur in non-disease proteins under partially unfavourable conditions or when the cellular interaction partners are absent. Reduction of the poly(Q) length brings oligomerization rates into an experimentally accessible time-window, allowing us to capture the early stages of the elongation phase of the mature ataxin-3 amyloid fibrils. The search for the pathogenic protein aggregates has practical implications because their formation and the proteins with which they interact are potential targets for therapeutic intervention. Thus, studying the aggregation pathway of non-expanded ataxin-3 will provide important clues about the early

aggregation mechanisms in MJD. Moreover, as we can monitor the formation of the amyloid precursors, which includes the isolation of early oligomers, we are now able to screen drugs that may interfere with the aggregation process and even identify at which stage of the polymerization they act.

Materials and Methods

Plasmid construction

A construct encoding the human ataxin-3 cDNA corresponding to the splice variant MJD1-1 (Swiss-Prot P54252_2, variant VSP_002784) has been described.[25] The EST clone yk77c4 (kindly provided by Yuji Kowara) corresponding to *C. elegans* mjd-1 cDNA was sequenced and its missing 5′ end completed using the RACE system (Gibco) following the manufacturer's instructions. The cDNA was obtained from total RNA using random primers. The PCR reaction was performed using the reverse primer ceNde 5′-GCA CAA ACC AGT GCT CTC TGA G-3′ and SL1 primer (spliced leader) with an additional PstI restriction site 5′-GAG GCT GCA GGT TTA ATT ACC CAA GTT TGA G-3′. The fragment was subcloned into the NdeI and PstI restriction sites of the initial yk77c4 construct and the full-length cDNA plasmid obtained (ceMJD) was confirmed by sequencing.

The full-length cDNAs encoding *MJD* gene splice variant MJD1-1, and the *C. elegans* orthologue protein were first amplified by PCR using primers including the 5′ and 3′ attB site-specific recombination sequences (Gateway Cloning System, Invitrogen Life Technologies) attB1-MJD (5′-GGG GAC AAG TTT GTA CAA AAA AGC AGG CTG GAT GGA GTC CAT CTT CCA CGA G-3′)/attB2-MJD1-1 (5′-GGG GAC CAC TTT GTA CAA GAA AGC TGG GTC TTA TTT TTT TCC TTC TGT TTT 3′), attB1-ceMJD (5′-GGG GAC AAG TTT GTA CAA AAA AGC AGG CTG GAT GTC AAA AGA CGA TCC GAT C-3′)/attB2-ceMJD (5′-GGG GAC CAC TTT GTA CAA GAA AGC TGG GTC TTA TTT TTC ATC GTT CCT CTC-3′). These attB-PCR products were cloned into pDONR201 vectors (Invitrogen Life Technologies), and the latter subcloned into pDEST17 expression vectors through site-specific recombination, using the Gateway Cloning System, according to the manufacturer's protocol.

Plasmid pDEST17-J1, encoding the catalytic Josephin domain of human ataxin-3, was obtained by introduction of a stop codon mutation at position 548–550 in the open reading frame, through QuickChange Site-Directed Mutagenesis (Stratagene). The mutagenesis primers were: Jos-1_For: 5′CGA AGC TGA CCA ACT CCT ACA GAT GAT TAG GTG ACA ACA GAT GCC TCG ACC3′ and Jos-1_Rev: 5′GGT CGA GGC ATC TGT TGT CAC CTA ATC ATC TGT AGG AGT TGG TCA GCT TCG3′. All bacterial expression constructs were verified by restriction enzyme digestion and automatic sequencing.

Protein expression and purification

The hexahistidine-tagged proteins were expressed in *E. coli* BL21(DE3)-SI cells (Invitrogen Life Technologies). Cells were grown at 37 °C in Luria broth medium without NaCl containing 100 mg/l of ampicillin and 0.2% (w/v) glucose. When cultures reached an absorbance at 600 nm of 0.5–0.7, expression of the fusion protein was induced by adding NaCl to a final concentration of 300 mM. After 3–4 h induction at 30 °C, the cells were collected by centrifugation, resuspended in cell lysis buffer L (25 mM sodium phosphate (pH 7.5), 500 mM NaCl, 10 mM imidazole) containing 50 mg/l of lysozyme and frozen at −20 °C. Before purification, a protease inhibitor cocktail (Complete EDTA-free, Roche) was added to the protein extract, and the supernatant obtained after centrifugation was applied to a HisTrap chelating column (Amersham Biosciences) and eluted in three steps by addition of buffer L containing 50 mM, 100 mM and 500 mM imidazole. Fractions suitable for further purification were selected by SDS-PAGE analysis. The fractions eluting after metalloaffinity chromatography (~10 ml) were applied to a Hiprep 26/60 column equilibrated in buffer A (20 mM Hepes (pH 7.5), 200 mM NaCl, 5% (v/v) glycerol) and eluted with a flow rate of 0.5 ml/min at 6 °C. The eluted proteins were monitored at 280 nm and compared to the elution profile of the following molecular mass standards: blue dextran (2000 kDa), 87.4 ml; thyroglobulin (669 kDa), 87.81 ml; ferritin (440 kDa), 90.02 ml; catalase (232 kDa), 104.3 ml; aldolase (158 kDa), 106.5 ml; bovine serum albumin (67 kDa), 125.3 ml; ovalbumin (43 kDa), 138.9 ml; and chymotrypsinogen A (25 kDa), 173.8 ml. After analysis by SDS-PAGE, and analytical gel-filtration chromatography (Superose 12 10/300 GL) the purest fractions were pooled and concentrated on Vivaspin15 concentrators (cutoff 10 kDa, Vivascience, Sartorius) to 2–10 mg/ml, immediately frozen in liquid nitrogen and stored at −80 °C. Protein concentrations were determined by measuring the absorbance at 280 nm using extinction coefficients of 36,160 $M^{-1}\,cm^{-1}$, 34,640 $M^{-1}\,cm^{-1}$ and 34,760 $M^{-1}\,cm^{-1}$ for human ataxin-3, *C. elegans* ataxin-3 and the Josephin domain, respectively.

In order to confirm purity after concentration, 50 μl of each concentrated ataxin-3 sample was applied on a Superose 12 10/300 GL column (Amersham Biosciences) equilibrated in buffer A, at room temperature. The gel-filtration column was calibrated with gel-filtration standard proteins (Amersham Biosciences), with the following elution volumes: thyroglobulin (669 kDa), 8.65 ml; aldolase (158 kDa), 11.72 ml; bovine serum albumin (67 kDa), 12.67 ml; ovalbumin (43 kDa), 13.54 ml; chymotrypsinogen A (25 kDa), 15.20 ml; ribonuclease A (13.7 kDa), 15.69 ml. The void volume of the column was determined by applying blue dextran, which eluted at 8.21 ml. The apparent molecular mass values (M_{app}) were calculated from an interpolation of a semi-log plot of partition coefficient (K_{av}) of the protein standards *versus* molecular mass.

Crosslinking with glutaraldehyde

A sample (10 μl) of 0.1 mg/ml of purified protein in buffer A was mixed with a freshly prepared 0.02% (v/v) glutaraldehyde solution, and incubated at room temperature. The reactions were allowed to proceed for 1 min, 5 min, 10 min and 20 min, and stopped by addition of 10 μl of 2× SDS sample buffer, followed by heating to 100 °C for 5 min. Samples were analyzed by SDS-PAGE.

Thioflavin-T staining

This assay is based on a previously described protocol.[59] Briefly, ThT (final concentration 30 μM) was added to 100 μg of protein in 50 mM glycine/NaOH buffer (pH 9.0), in an assay volume of 1 ml. Excitation and emission slits were set at 5 nm and 10 nm, respectively.

The excitation spectra (400–500 nm) were recorded by spectrofluorimetry (FP-770; JASCO) at 25 °C with emission recorded at 482.0 nm.

Fibril formation and seeding effects monitored by the ThT fluorescence assay

Series of solutions (1 ml) of human ataxin-3 (14Q) were prepared (0.3 mg/ml) in buffer B (20 mM Hepes (pH 7.5), 200 mM NaCl, 5 mM EDTA, 1 mM DTT, 1 mM PMSF). Solutions of monomers, monomers plus preformed dimeric species (4%, w/w) and monomers plus HMM soluble oligomers (10%, w/w), were incubated at 37 °C along with a blank buffer solution. ThT fluorescence was monitored over a period of 90 h in a SPECTRAmax microplate spectrofluorimeter at 37 °C. The fluorescence measurements were performed as follows. At increasing incubation times, 100 μl of the protein solutions and of the blank buffer solution were added to 150 μl of 16.7 μM ThT in 50 mM glycine/NaOH buffer (pH 9.0) (ThT final concentration 10 μM). The fluorescence was measured immediately setting the excitation wavelength to 440 nm and collecting the emission at 482 nm. The values obtained for the protein solutions were corrected with the blank buffer reading.

Circular dichroism

Synchrotron Radiation CD spectra were collected on beam line CD12 of the CLRC Daresbury Laboratory's Synchrotron Radiation Source (SRS). Spectrosil cuvettes of 0.05 mm, 0.02 mm and 0.01 mm pathlengths were used with protein samples at concentrations of 2.1–12.6 mg/ml in buffer A. The spectra were measured at 4 °C between 170 nm and 260 nm, corrected with a blank buffer reading and scaled to molar ellipticity using the CD spectrum of (+)-10-camphorsulfonic acid at 1 mg/ml. The analysis of the secondary structure content was performed with Contin, Selcon and CDsstr methods. Spectra deconvolution results were very consistent for the three methods although, for most spectra, the lowest experimental/calculated RMSD was achieved with the Contin method.

Congo red staining

Ataxin-3 soluble oligomers and aggregates were incubated for 20 min with 80% (v/v) ethanol saturated with NaCl followed by 1% (w/w) Congo red in 80% alkaline ethanol saturated with NaCl and left to dry onto microscopy slides. The samples were examined for birefringence under polarized light in an Olympus polarization light microscope.

Electron microscopy

EM images were acquired using a Zeiss (60 kV) electron microscope. For each experiment, 10 μl of protein solution was placed on a formvar and carbon-coated grid and blotted off after 5 min. The sample was then stained with 3 ml of (2%, w/v) uranyl acetate, dried and observed at a magnification of 10,000–25,000×.

Dot blot assay

Samples (1 μg) of HMM oligomers, multimers and monomers of the recombinant proteins were applied to a nitrocellulose membrane, blocked with non-fat milk in Tris-buffered saline (TBS) containing 0.01% (v/v) Tween 20 (TBS-T), at room temperature for 1 h, washed three times for 5 min each with TBS-T and incubated for 1 h at room temperature with the oligomer-specific antibody kindly provided by C.G. Glabe (0.1 μg/ml in 3% (w/v) BSA in TBS-T)[16] or with the anti-His antibody (Amersham Biosciences) (1:10,000 (v/v) in 3% BSA in TBS-T). The membranes were washed three times for 5 min each with TBS-T, incubated with alkaline-phosphatase conjugated anti-rabbit IgG or anti-mouse IgG (Amersham-Pharmacia) diluted 1:10,000 (v/v) in 3% BSA in TBS-T and incubated for 1 h at room temperature. The blots were washed three times for 5 min each with TBS-T and developed with the ECF kit (Amersham Biosciences).

Acknowledgements

This work was supported by Fundação para a Ciência e a Tecnologia, Portugal (Project POCTI/MGI/47550/2002, co-financed by FEDER), by Fundação Luso-Americana para o Desenvolvimento and by the National Ataxia Foundation. The authors acknowledge R. Fernandes for excellent technical assistance in TEM, P. J. B. Pereira for critical reading of the manuscript, and E. Pires for continuous support. We thank R. Kayed and C. G. Glabe for the generous gift of the anti-oligomer antibody.

Supplementary Data

Supplementary data associated with this article can be found, in the online version, at doi:10.1016/j.jmb.2005.08.061

References

1. Cummings, C. J. & Zoghbi, H. Y. (2000). Fourteen and counting: unraveling trinucleotide repeat diseases. *Hum. Mol. Genet.* **9**, 909–916.
2. Perutz, M. (1994). Polar zippers: their role in human disease. *Protein Sci.* **3**, 1629–1637.
3. Rubinsztein, D. C., Wyttenbach, A. & Rankin, J. (1999). Intracellular inclusions, pathological markers in diseases caused by expanded polyglutamine tracts? *J. Med. Genet.* **36**, 265–270.
4. Perutz, M. F., Johnson, T., Suzuki, M. & Finch, J. T. (1994). Glutamine repeats as polar zippers: their possible role in inherited neurodegenerative diseases. *Proc. Natl Acad. Sci. USA*, **91**, 5355–5358.
5. Masino, L. & Pastore, A. (2002). Glutamine repeats: structural hypotheses and neurodegeneration. *Biochem. Soc. Trans.* **30**, 548–551.
6. Chen, S., Berthelier, V., Hamilton, J. B., O'Nuallain, B. & Wetzel, R. (2002). Amyloid-like features of polyglutamine aggregates and their assembly kinetics. *Biochemistry*, **41**, 7391–7399.
7. Scherzinger, E., Lurz, R., Turmaine, M., Mangiarini, L., Hollenbach, B., Hasenbank, R. *et al.* (1997). Huntingtin-encoded polyglutamine expansions form amyloid-like protein aggregates *in vitro* and *in vivo*. *Cell*, **90**, 549–558.

8. Bevivino, A. E. & Loll, P. J. (2001). An expanded glutamine repeat destabilizes native ataxin-3 structure and mediates parallel beta-fibrils. *Proc. Natl Acad. Sci. USA*, **98**, 11955–11960.
9. Poirier, M. A., Li, H., Macosko, J., Cai, S., Amzel, M. & Ross, C. A. (2002). Huntingtin spheroids and protofibrils as precursors in polyglutamine fibrilization. *J. Biol. Chem.* **277**, 41032–41037.
10. McGowan, D. P., van Roon-Mom, W., Holloway, H., Bates, G. P., Mangiarini, L., Cooper, G. J. S. *et al*. (2000). Amyloid-like inclusions in Huntington's disease. *Neuroscience*, **100**, 677–680.
11. O'Nuallain, B. & Wetzel, R. (2002). Conformational Abs recognizing a generic amyloid fibril epitope. *Proc. Natl Acad. Sci. USA*, **99**, 1485–1490.
12. Michalik, A. & Van Broeckhoven, C. (2003). Pathogenesis of polyglutamine disorders: aggregation revisited. *Hum. Mol. Genet.* **12**, R173–R186.
13. Iuchi, S., Hoffner, G., Verbeke, P., Djian, P. & Green, H. (2003). Oligomeric and polymeric aggregates formed by proteins containing expanded polyglutamine. *Proc. Natl Acad. Sci. USA*, **100**, 2409–2414.
14. Tanaka, M., Machida, Y., Nishikawa, Y., Akagi, T., Hashikawa, T., Fujisawa, T. & Nukina, N. (2003). Expansion of polyglutamine induces the formation of quasi-aggregate in the early stage of protein fibrillization. *J. Biol. Chem.* **278**, 34717–34724.
15. Tycko, R. (2004). Progress towards a molecular-level structural understanding of amyloid fibrils. *Curr. Opin. Struct. Biol.* **14**, 96–103.
16. Kayed, R., Head, E., Thompson, J. L., McIntire, T. M., Milton, S. C., Cotman, C. W. & Glabe, C. G. (2003). Common structure of soluble amyloid oligomers implies common mechanism of pathogenesis. *Science*, **300**, 486–489.
17. Kayed, R., Sokolov, Y., Edmonds, B., McIntire, T. M., Milton, S. C., Hall, J. E. & Glabe, C. G. (2004). Permeabilization of lipid bilayers is a common conformation-dependent activity of soluble amyloid oligomers in protein misfolding diseases. *J. Biol. Chem.* **279**, 46363–46366.
18. Paulson, H. L., Das, S. S., Crino, P. B., Perez, M. K., Patel, S. C., Gotsdiner, D. *et al*. (1997). Machado-Joseph disease gene product is a cytoplasmic protein widely expressed in brain. *Ann. Neurol.* **41**, 453–462.
19. Burnett, B., Li, F. & Pittman, R. N. (2003). The polyglutamine neurodegenerative protein ataxin-3 binds polyubiquitylated proteins and has ubiquitin protease activity. *Hum. Mol. Genet.* **12**, 3195–3205.
20. Burnett, B. G. & Pittman, R. N. (2005). The polyglutamine neurodegenerative protein ataxin 3 regulates aggresome formation. *Proc. Natl Acad. Sci. USA*, **102**, 4330–4335.
21. Chai, Y., Berke, S. S., Cohen, R. E. & Paulson, H. L. (2004). Poly-ubiquitin binding by the polyglutamine disease protein ataxin-3 links its normal function to protein surveillance pathways. *J. Biol. Chem.* **279**, 3605–3611.
22. Warrick, J. M., Morabito, L. M., Bilen, J., Gordesky-Gold, B., Faust, L. Z., Paulson, H. L. & Bonini, N. M. (2005). Ataxin-3 suppresses polyglutamine neurodegeneration in Drosophila by a ubiquitin-associated mechanism. *Mol. Cell.* **18**, 37–48.
23. Masino, L., Musi, V., Menon, R. P., Fusi, P., Kelly, G., Frenkiel, T. A. *et al*. (2003). Domain architecture of the polyglutamine protein ataxin-3: a globular domain followed by a flexible tail. *FEBS Letters*, **549**, 21–25.
24. Scheel, H., Tomiuk, S. & Hofmann, K. (2003). Elucidation of ataxin-3 and ataxin-7 function by integrative bioinformatics. *Hum. Mol. Genet.* **12**, 2845–2852.
25. Goto, J., Watanabe, M., Ichikawa, Y., Yee, S. B., Ihara, N., Endo, K. *et al*. (1997). Machado-Joseph disease gene products carrying different carboxyl termini. *Neurosci. Res.* **28**, 373–377.
26. Maciel, P., Gaspar, C., DeStefano, A. L., Silveira, I., Coutinho, P., Radvany, J. *et al*. (1995). Correlation between CAG repeat length and clinical features in Machado-Joseph disease. *Am. J. Hum. Genet.* **57**, 54–61.
27. Shehi, E., Fusi, P., Secundo, F., Pozzuolo, S., Bairati, A. & Tortora, P. (2003). Temperature-dependent, irreversible formation of amyloid fibrils by a soluble human ataxin-3 carrying a moderately expanded polyglutamine stretch (Q36). *Biochemistry*, **42**, 14626–14632.
28. Marchal, S., Shehi, E., Harricane, M. C., Fusi, P., Heitz, F., Tortora, P. & Lange, R. (2003). Structural instability and fibrillar aggregation of non-expanded human ataxin-3 revealed under high pressure and temperature. *J. Biol. Chem.* **278**, 31554–31563.
29. Chow, M. K., Paulson, H. L. & Bottomley, S. P. (2004). Destabilization of a non-pathological variant of ataxin-3 results in fibrillogenesis *via* a partially folded intermediate: a model for misfolding in polyglutamine disease. *J. Mol. Biol.* **335**, 333–341.
30. Chai, Y., Wu, L., Griffin James, D. & Paulson Henry, L. (2001). The role of protein composition in specifying nuclear inclusion formation in polyglutamine disease. *J. Biol. Chem.* **276**, 44889–44897.
31. Masino, L., Nicastro, G., Menon, R. P., Piaz, F. D., Calder, L. & Pastore, A. (2004). Characterization of the structure and the amyloidogenic properties of the josephin domain of the polyglutamine-containing protein ataxin-3. *J. Mol. Biol.* **344**, 1021–1035.
32. Cardoso, I., Goldsbury, C. S., Muller, S. A., Olivieri, V., Wirtz, S., Damas, A. M. *et al*. (2002). Transthyretin fibrillogenesis entails the assembly of monomers: a molecular model for *in vitro* assembled transthyretin amyloid-like fibrils. *J. Mol. Biol.* **317**, 683–695.
33. Rochet, J. C., Conway, K. A. & Lansbury, P. T., Jr (2000). Inhibition of fibrillization and accumulation of prefibrillar oligomers in mixtures of human and mouse alpha-synuclein. *Biochemistry*, **39**, 10619–10626.
34. Chen, S., Ferrone, F. A. & Wetzel, R. (2002). Huntington's disease age-of-onset linked to polyglutamine aggregation nucleation. *Proc. Natl Acad. Sci. USA*, **99**, 11884–11889.
35. Chen, S., Berthelier, V., Yang, W. & Wetzel, R. (2001). Polyglutamine aggregation behavior *in vitro* supports a recruitment mechanism of cytotoxicity. *J. Mol. Biol.* **311**, 173–182.
36. Chow, M. K., Ellisdon, A. M., Cabrita, L. D. & Bottomley, S. P. (2004). Polyglutamine expansion in ataxin-3 does not affect protein stability: Implications for misfolding and disease. *J. Biol. Chem.* **279**, 47643–47651.
37. Demuro, A., Mina, E., Kayed, R., Milton, S. C., Parker, I. & Glabe, C. G. (2005). Calcium dysregulation and membrane disruption as a ubiquitous neurotoxic mechanism of soluble amyloid oligomers. *J. Biol. Chem.* **280**, 17294–17300.
38. Stefani, M. & Dobson, C. M. (2003). Protein aggregation and aggregate toxicity: new insights into protein folding, misfolding diseases and biological evolution. *J. Mol. Med.* **81**, 678–699.
39. Stott, K., Blackburn, J. M., Butler, P. J. G. & Perutz, M. (1995). Incorporation of glutamine repeats makes

protein oligomerize - implications for neurodegenerative diseases. *Proc. Natl Acad. Sci. USA*, **92**, 6509–6513.
40. Chen, Y. W., Stott, K. & Perutz, M. F. (1999). Crystal structure of a dimeric chymotrypsin inhibitor 2 mutant containing an inserted glutamine repeat. *Proc. Natl Acad. Sci. USA*, **96**, 1257–1261.
41. Duncan, J. G., Carbajo, R. J., Stott, K. & Neuhaus, D. (2001). Solution studies of chymotrypsin inhibitor-2 glutamine insertion mutants show no interglutamine interactions. *Biochem. Biophys. Res. Commun.* **280**, 855–860.
42. Bennett, M. J. & Eisenberg, D. (2004). The evolving role of 3D domain swapping in proteins. *Structure*, **12**, 1339–1341.
43. Jaskolski, M. (2001). 3D domain swapping, protein oligomerization, and amyloid formation. *Acta Biochim. Pol.* **48**, 807–827.
44. Burright, E. N., Davidson, J. D., Duvick, L. A., Koshy, B., Zoghbi, H. Y. & Orr, H. T. (1997). Identification of a self-association region within the SCA1 gene product, ataxin-1. *Hum. Mol. Genet.* **6**, 513–518.
45. de Chiara, C., Menon, R. P., Adinolfi, S., de Boer, J., Ktistaki, E., Kelly, G. *et al*. (2005). The AXH domain adopts alternative folds the solution structure of HBP1 AXH. *Structure*, **13**, 743–753.
46. Fernandez-Funez, P., Nino-Rosales, M. L., de Gouyon, B., She, W. C., Luchak, J. M., Martinez, P. *et al*. (2000). Identification of genes that modify ataxin-1-induced neurodegeneration. *Nature*, **408**, 101–106.
47. Fan, X., Dion, P., Laganiere, J., Brais, B. & Rouleau, G. A. (2001). Oligomerization of polyalanine expanded PABPN1 facilitates nuclear protein aggregation that is associated with cell death. *Hum. Mol. Genet*, **10**, 2341–2351.
48. Paulson, H. (2003). Polyglutamine neurodegeneration: minding your Ps and Qs. *Nature Med.* **9**, 825–826.
49. Chen, S., Ferrone Frank, A. & Wetzel, R. (2002). Huntington's disease age-of-onset linked to polyglutamine aggregation nucleation. *Proc. Natl Acad. Sci. USA*, **99**, 11884–11889.
50. Harper, J. D. & Lansbury, P. T., Jr (1997). Models of amyloid seeding in Alzheimer's disease and scrapie: mechanistic truths and physiological consequences of the time-dependent solubility of amyloid proteins. *Annu. Rev. Biochem.* **66**, 385–407.
51. Bucciantini, M., Giannoni, E., Chiti, F., Baroni, F., Formigli, L., Zurdo, J. *et al*. (2002). Inherent toxicity of aggregates implies a common mechanism for protein misfolding diseases. *Nature*, **416**, 507–511.
52. Walsh, D. M. & Selkoe, D. J. (2004). Oligomers on the brain: the emerging role of soluble protein aggregates in neurodegeneration. *Protein Pept. Letters*, **11**, 213–228.
53. Schaffar, G., Breuer, P., Boteva, R., Behrends, C., Tzvetkov, N., Strippel, N. *et al*. (2004). Cellular toxicity of polyglutamine expansion proteins: mechanism of transcription factor deactivation. *Mol. Cell.* **15**, 95–105.
54. Kazlauskaite, J., Young, A., Gardner, C. E., Macpherson, J. V., Venien-Bryan, C. & Pinheiro, T. J. (2005). An unusual soluble beta-turn-rich conformation of prion is involved in fibril formation and toxic to neuronal cells. *Biochem. Biophys. Res. Commun.* **328**, 292–305.
55. Arrasate, M., Mitra, S., Schweitzer, E. S., Segal, M. R. & Finkbeiner, S. (2004). Inclusion body formation reduces levels of mutant huntingtin and the risk of neuronal death. *Nature*, **431**, 805–810.
56. Fujigasaki, H., Uchihara, T., Koyano, S., Iwabuchi, K., Yagishita, S., Makifuchi, T. *et al*. (2000). Ataxin-3 is translocated into the nucleus for the formation of intranuclear inclusions in normal and Machado-Joseph disease brains. *Expt. Neurol.* **165**, 248–256.
57. Fujigasaki, H., Uchihara, T., Takahashi, J., Matsushita, H., Nakamura, A., Koyano, S. *et al*. (2001). Preferential recruitment of ataxin-3 independent of expanded polyglutamine: an immunohistochemical study on Marinesco bodies. *J. Neurol. Neurosurg. Psychiatry*, **71**, 518–520.
58. Lieberman, A. P., Trojanowski, J. Q., Leonard, D. G., Chen, K. L., Barnett, J. L., Leverenz, J. B. *et al*. (1999). Ataxin 1 and ataxin 3 in neuronal intranuclear inclusion disease. *Ann. Neurol.* **46**, 271–273.
59. Gales, L., Cardoso, I., Fayard, B., Quintanilha, A., Saraiva, M. J. & Damas, A. M. (2003). X-ray absorption spectroscopy reveals a substantial increase of sulfur oxidation in transthyretin (TTR) upon fibrillization. *J. Biol. Chem.* **278**, 11654–11660.
60. Poirot, O., O'Toole, E. & Notredame, C. (2003). Tcoffee@igs: a web server for computing, evaluating and combining multiple sequence alignments. *Nucl. Acids Res.* **31**, 3503–3506.
61. Barton, G. J. (1993). ALSCRIPT: a tool to format multiple sequence alignments. *Protein Eng.* **6**, 37–40.

Edited by F. E. Cohen

(Received 4 June 2005; received in revised form 16 August 2005; accepted 25 August 2005)
Available online 12 September 2005